Second International Conference on CFD in the Minerals and Process Industries
CSIRO, Melbourne, Australia
6-8 December 1999

ANALYSIS OF GAS FLOW AND MIXING IN A ROTARY KILN WASTE INCINERATOR

Y. YANG, J. RAKHORST, M. A. REUTER, J. H.L. VONCKEN

Department of Raw Materials Processing
Applied Earth Sciences, Delft University of Technology
Mijnbouwstraat 120, 2628 RX Delft, THE NETHERLANDS
Email: Y.Yang@ta.tudelft.nl Internet: http://www.ta.tudelft.nl

ABSTRACT

Rotary kiln incinerators are widely used in the treatment of liquid and solid hazardous wastes. However, the complex transport and chemical processes within the system are still not well understood. The refractory failure caused by liquid slag attack is related to the gas flow and gas temperature distributions. The current paper describes the gas flow and mixing behaviour in an industrial rotary kiln incinerator for disposing hazardous wastes, by using a general purpose CFD-code PHOENICS. The results indicate that the gas flow and mixing inside the kiln is very complicated. The 3-dimensional gas flow will help to better understand the heterogeneous temperature distribution inside the kiln, which will affect significantly the bed behaviour and refractory lining wear. In the future, heat transfer within the kiln will be included in this research. The numerical predictions will provide useful information for improved process control.

INTRODUCTION

Various incineration technologies are available for handling different types of hazardous wastes, such as rotary kiln, fixed hearth, and fluidised bed incinerators. The rotary kiln incineration system is regarded to be the most versatile for its ability to handle solid, liquid, and sludge wastes at a high throughput. Figure 1 illustrates a layout of the rotary-kiln incineration system for hazardous wastes used at AVR Chemie, and Figure 2 shows a closer view of the rotary kiln.

The rotary kiln forms the primary combustion chamber, being a steel cylinder lined with refractory bricks for insulation and protection against slag attacks. The cylinder is mounted at an angle of 1-2° from the horizontal and rotates at a speed of 0.2 to 0.3 rpm. In combination with a secondary combustion chamber, waste-heat recovery boiler, and flue-gas cleaning system, rotary kiln incinerators have been widely used as a thermal treatment system integrated into an industrial complex to recover energy from wastes (Sigg, 1991).

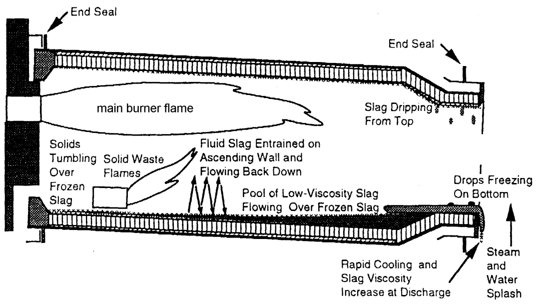

Figure 2: Illustration of the rotary kiln (Veranth, et al., 1996).

Although the rotary kiln incinerators are routinely being used in the treatment of liquid/solid hazardous wastes, the complex transport and chemical processes occurring within these systems are not well understood (Leger et al., 1993). The operation of industrial kilns has been an art learned by experience. The system is normally over-designed and operates well below the regulatory emission limits, but at a cost of capital and fuel. The refractory failure caused by liquid slag attack leads to frequent downtime and high cost for relining the system. If the processes governing the destruction of waste within the kiln can be well characterised and modelled, improvements in performance and economics of the rotary kiln incinerator may be realised.

The thermal behaviour of the kiln is strongly affected by the fluid-dynamics of the combustion gas in the kiln: gas flow and mixing pattern, and the energy and temperature

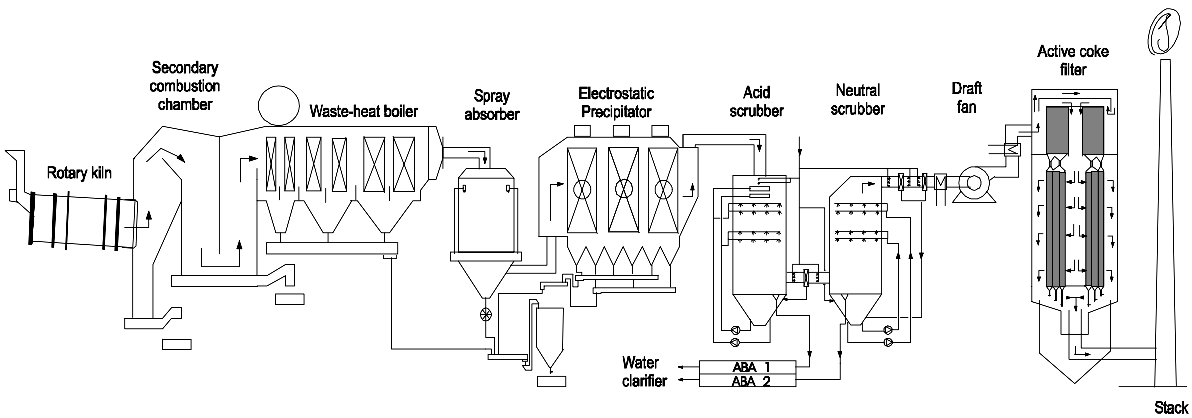

Figure 1: A general layout of an incineration facility used at AVR Chemie, the Netherlands.

distributions. The strong inter-coupling of gas flow and heat transfer process with the thermal behaviour of the formed slag layer and the refractory lining, encourages detailed studies on the transport phenomena of the gas phase: the gas flow and heat transfer inside the rotary kiln. Computational Fluid-dynamics (CFD) modelling provides a convenient tool in giving more insights within the kiln. CFD has the capability to incorporate almost all aspects of the process, including combustion kinetics. A great advantage of CFD modelling is the substantial savings in cost and time in comparison to the experimental studies for scale-up, if a reliable model is established.

For CFD modelling of rotary kiln incinerators, a number of studies can be found in the literature, but very little have been related to the systems with solid waste-incineration. Leger et al. (1993) developed a model for methane combustion to investigate the importance of turbulence air injection and leakage air location, without taking waste-combustion and thermal radiation into account. Khan and Morse (1993) reported the CFD modelling of a rotary kiln waste incinerator with a global one-step reaction for CH4 combustion, neglecting the radiative heat transfer. Jakway et al. (1996) developed further the CFD model of the rotary kiln after Leger et al. (1993) by including thermal radiation, but the model was still limited to CH4 without solid waste processing. Veranth et al. (1997) modelled the temperature distribution in a hazardous waste slagging rotary kiln, and their focus was on the correlation between the gas, wall and the bed temperatures. Thermal radiation was included with the S-4 discrete-ordinate method. Wardenier and Van den Bulck (1997) developed a model where evolution of cellulose and toluene from a solid bed is considered. The study included the investigation on the effects of geometry, overall configuration and optimal operating parameters.

AVR-Chemie, located at the Rotterdam harbour, specialises in the thermal destruction of hazardous wastes, and operates two rotary kiln incinerators for hazardous chemical wastes. Over the past few years various studies have been conducted at Delft University of Technology to extend the lifetime of the refractory lining inside the rotary kiln in co-operation with AVR Chemie. A recent project with AVR Chemie includes further experimental study on novel slag layer composition for refractory protection and CFD modelling of gas flow and heat transfer in the rotary kiln for hazardous waste incineration. The current paper describes the preliminary modelling results: gas flow and mixing under non-isothermal conditions. Detailed radiative heat transfer simulation and simple combustion modelling are being included soon. The final objective is to provide possibilities for better understanding the aerodynamic and thermal behaviour of the kiln, reducing the refractory lining wear of the kiln, and gaining better overall control of the incineration process.

MODEL DESCRIPTION

The physical system

The incineration system of the current study is a standard type of industrial-scale rotary kiln waste-incinerator operated at AVR Chemie, as illustrated in Figure 1. The rotary kiln is 4.2 m in diameter and 11.4 m in length, at an inclination angle of 2°, and with a rotation speed of 0.2-0.3 rpm. In the system, the rotary kiln is followed by a secondary combustion chamber, a waste-heat boiler, and a flue-gas cleaning system including a spray absorber, an electrostatic precipitator, two wet scrubbers and an active coke filter. At the charge end, the feed system consists of a main burner, a sludge burner, and the load chute.

A wide range of hazardous wastes is incinerated in the rotary kiln system. The first type of wastes consists of high caloric waste such as waste oil and solvents, with an average caloric value of roughly 30 MJ/kg. It is fed into a main burner, located at the front end of the rotary kiln where it is mixed with combustion air before entering the kiln. The second type of waste is low caloric waste with an averages caloric value of 9 - 10 MJ/kg, which may contain any kind of organic solution with 40% organic content on average. It is normally burned at the secondary combustion chamber. The third type of waste consists of bulk solids or anything filled in a container (liquid or solid), which is normally fed though the load chute, and burned inside the kiln after breaking down and forming a bed at the bottom of the kiln, supported by the main burner flame. Some sludges are burned through a sludge burner. The thermal rating of the waste-incinerator is around 25 –30 MW.

Simulation tool

The gas flow and mixing behaviour is simulated with a commercial CFD package PHOENICS (3.1 and 3.2). PHOENICS is a finite volume CFD code for solving transport equations of mass, momentum and energy conservation. The partial differential equations governing the gas flow and heat transfer can be expressed by a generalised time-averaged transport equation:

$$\frac{\partial}{\partial t}(\rho\phi) + div(\rho\mathbf{u}\phi) = div(\Gamma_{\phi,eff}\ grad\ \phi) + S_\phi \qquad (1)$$

Where ϕ is the general flow variable such as velocity components, temperature, or mass fractions etc.; ρ is the fluid density; $\mathbf{u}$ is the fluid velocity vector. The effects of fluid turbulence and radiative heat transfer are accounted for in the transport coefficient $\Gamma_{\phi,eff}$ and source term S_ϕ by a turbulence model and a radiation model.

According to the evaluation of the Reynolds numbers at the burners (140,000 – 170,000) and load chute (~50,000) and the within the cylindrical part of the kiln (average ~70,000), the general flow regime inside the kiln is turbulent. To take into account the turbulent effect, both the standard k-ε model and two modified k-ε models of RNG k-ε (Yakhot et al., 1992) and Chen-Kim k-ε (Chen and Kim, 1987) were utilised. Comparisons of different model results are made. In order to account for the gas cooling effect on the flow conditions, both adiabatic mixing and gas phase convection-radiation were considered. A composite-flux model (Spalding 1980) and Immersol radiation model (CHAM, 1999) supplied with PHOENICS were used in simulation, and the latter is more thoroughly used in heat transfer models.

Simulation approach and assumptions

Due to the complexity of the incineration process within the rotary kiln, especially the wide range of waste types and the complicated combustion processes, assumptions have to be made, in order to construct a simulation model. Before combustion models are implemented into the simulation, the heat and mass sources were represented by two approximate approaches:

(1) As the first approximation, the wastes are assumed to be combusted before entering the kiln, so that hot combustion gas streams from the main burner (for high caloric waste), sludge burner and from the load chute (for solid or liquid waste in containers) mix and flow through the kiln. The gas flow behaviour is studied under conditions of both adiabatic mixing and heat transfer including radiation.
(2) The wastes from containers are assumed to burn within the kiln after breaking down and forming a solid bed. The volumetric flow rate and an adiabatic temperature are evaluated and implemented in the model as the fourth inlet, according to the average processing capacity.

Additional assumptions in this study include:
(1) The process is assumed to be in steady state, which simulates the average operating conditions.
(2) The cyclic burning process of the container wastes is simplified to a steady and continuous process.

To represent the energy source from waste combustion, both the fixed temperatures (estimated from the adiabatic temperatures) and fixed volumetric/surface heat sources (estimated from calorimetric heat content of the wastes) were tested. Due to the extreme convergence difficulties in using fixed heat source, the fixed temperature approach was used more thoroughly.

Computational grid

In order to take into account the backward influences on the flow and heat transfer near the kiln exit plane, the geometry includes the rotary kiln and the transition zone to the secondary combustion chamber. To manage a cylindrical kiln and the rectangular transition zone, different attempts were made. BFC grid would be ideal to cope with this combination, however, the BFC grid generator in PHOENICS is still difficult to use, incompatible with its main user interface. On the other hand, a BFC grid normally causes more difficulties in convergence. Therefore, the Cartesian grid was used, and the cylindrical shape of the kiln was approximated with cell blocking technique. Figure 3 illustrates the model geometry which shows the conjunction between the cylindrical kiln and the secondary combustion chamber, and computational grid for the current study (55×20×27 =29,700), including the locations of the load chute, the main and sludge burners. The active cells are around 19,000.

In the model, the burner inlets were defined with rectangular shapes with the same effective areas as the circular burners, to get the same incoming velocities. A finer grid of 110×20×27 has also been tested, resulting in almost the same flow pattern as in the coarse grid. Since the definition of the burners does not allow larger cell sizes, at least in the Y-Z plane, a coarser grid was not tested. All the simulations were conducted with the coarse grid, and is regarded as grid independence.

Input and boundary conditions

The mass and energy inputs were obtained from AVR Chemie for average operating conditions. Tables 1 and 2 show the heat and mass input to the kiln system as well as adiabatic gas temperatures when the wastes are all combusted before entering the kiln. By subtracting 0.3 kg/s ash/slag formation from the total mass in-flow, the total mass flow rate in the gas phase was taken as 12.5 kg/s for making an overall heat and mass balance. The adiabatic (ideal) mixing temperature was estimated at 1250°C which is a reference temperature in operation, by taking into account 5% heat loss through kiln walls and 5% of heat loss into ashes and slags.

Locations	Air (kg/hr)	Waste (kg/hr)	Total (kg/hr)	Total (kg/s)
Load chute	27000	3000	30000	8.3
Main Burner	9000	1250	10250	2.9
Sludge Burner	5000	800	5800	1.6
Total	41000	5050	46050	12.8

Table 1. Estimation of mass flow rate into the rotary kiln.

Locations	Waste (MJ/kg)	Energy value (MW)	Adiabatic temp. (°C)
Load chute	13.4	11.2	920
Sludge Burner	13.4	3.0	1215
Main Burner	33.6	11.7	2470
Total		25.9	

Table 2. Estimation of energy input and adiabatic flame temperatures.

When a solid bed was used to approximate the combustion process of the solid waste, a certain amount of cold air at 25°C was assumed to enter the kiln through the load chute, and part of the air was distributed to the solid bed for combustion gas estimation. The estimated adiabatic flame temperature for the solid bed is then around 3157°C. Obviously, this approach will bring different flow and heat transfer results from the first approximation.

At the inlets of the burners, load chute, or solid bed, the turbulent intensity was set to 5%. The velocity components at different inlets were determined according to the effective area and the volume flow rate at the specified temperatures. The gas from load chute (air or pre-combusted off-gases) has an angle of 50° downward. The gas from the main burner has an angle of 5° towards the kiln axis, and the sludge burner has angles of 13.5° downward from the horizontal and 6° towards the kiln axis.

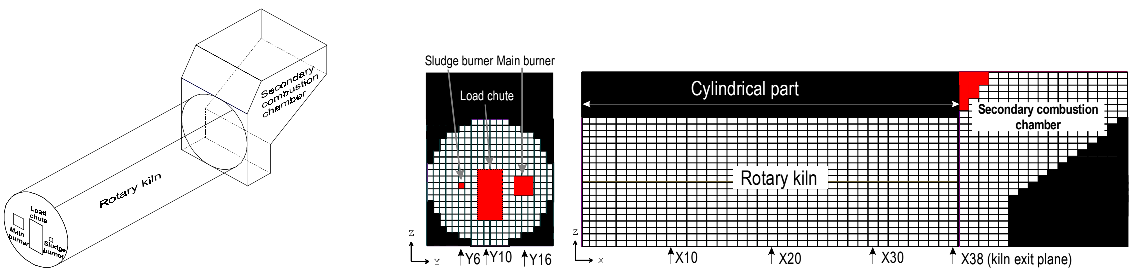

Figure 3: Model geometry and computational grid for the rotary kiln and part of the secondary combustion chamber.

For adiabatic mixing models, all walls are kept as adiabatic with equilibrium wall functions for friction. For the cases with convection-radiation heat transfer, the inner walls of the kiln were set at 1200°C, and the walls in the secondary combustion chamber were fixed as 1000°C. Wall emissivity was set at 0.8. The equilibrium log-law wall functions were used for friction and convection heat transfer. The kiln was assumed to be horizontal and stationary in the simulation, since the inclination angle of the kiln is small, and its rotation speed is low.

Thermophysical properties of the gas mixture

The thermophysical properties of the gas mixtures were evaluated according to the average off-gas compositions at the kiln outlet: 7.5% O_2, 9% H_2O, 14% CO_2 and 69.5% N_2. The properties were estimated as functions of temperature for the given gas composition. Table 3 shows the property data for the above given gas composition.

In order to see how much the property approximation affects the flow and heat transfer, average constant values of viscosity, heat capacity and thermal conductivity were also tested, and the difference in flow pattern is small.

Property	Formula
Density (kg/m^3):	ideal gas law: $p/(286.12T)$
Kinematic viscosity (m^2/s)	$-4.344\times10^{-6} +3.539\times10^{-8}T +8.267\times10^{-11}T^2$
Specific heat (J/kgK)	$1051+0.4304T-7.632\times10^{-5}T^2$
Thermal conductivity	$6.2853\times10^{-3}+6.2656\times10^{-5}T$

p - absolute pressure (Pa); *T* - absolute temperature (K).

Table 3. Estimated thermophysical properties of the gas mixture as functions of temperature.

RESULTS AND DISCUSSION

Gas flow and mixing behaviour inside the rotary kiln plays an important role in combustion efficiency and temperature homogeneity. In this study, three types of simulations were conducted.

(1) **Flame-jet models**: The chemical combustion processes are assumed to be complete before the air and wastes enter the kiln, which corresponds to the first approach described previously. Hot combusted gases flow into the kiln through the load chute, the main burner, and the sludge burner at different temperatures.

(2) **Solid-bed models**: The solid/liquid wastes in containers are assumed to combust within the kiln after breaking down and forming a solid bed. An extra inlet of mass and energy is defined. Air is redistributed between the load chute and the solid bed.

(3) **Turbulent model tests**: The comparison of different turbulent models was conducted for flame-jet models. Since the result differences from different models are not large, further tests were not extended to the solid-bed models.

Flame-jet models

Flame-jet models give a general idea how the different gas streams are mixed upon entering the kiln at relatively different temperatures. Figure 4 illustrates the general gas flow pattern at a few essential locations. Downward flow from load chute causes a large backward recirculating flow in the upper part of the kiln. A large swirl can be noticed above the jet streams. Near the kiln bottom, a clear rapid forward flow can be observed. Looking through the cross-sections along the kiln axis, a very asymmetric flow pattern can be seen, due to the two slightly inward jets from the burners toward the kiln axis. A clear counter clock-wise swirl was formed even from the middle of the kiln, viewing from the discharge end.

Figure 5 shows the distribution of the species from the load chute. Because the gas stream from the sludge burner was directed towards the kiln axis and the bottom, the gas from the load chute was clearly driven to the kiln wall on the main-burner side. This may cause the less mixing of the low temperature stream from the load chute with high temperature streams from the burners. This model showed a poor mixing among the three gas-streams. However, the gas volume and the temperature from the load chute are over estimated in this approach.

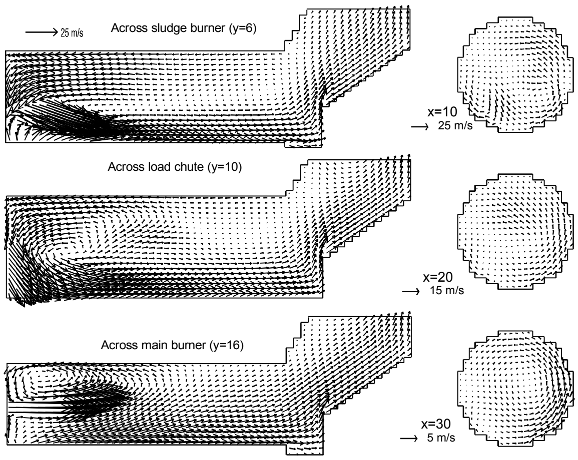

Figure 4: Velocity distribution in the flame-jet model.

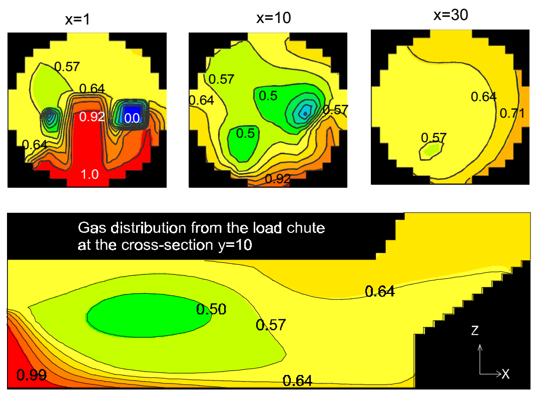

Figure 5: Species distribution of the gas from the load chute.

When radiative heat transfer is included in a non-adiabatic mixing model, the general flow pattern and the mixing behaviour of different streams, as well as the temperature distribution pattern, are still maintained.

Solid-bed models

Compared to the flame-jet models, the solid–bed models give a better approximation to the combustion of the container wastes. Though real combustion reactions are not included, the combusted hot off-gases from the formed solid-bed will give a good indication of the flow behaviour near that region. Figure 6 illustrates the calculated gas flow pattern across the burner and chute areas. A clear upward gas flow from the solid-bed can be observed. Together with the reduced gas volume and the much lower gas temperature at the load chute (25°C), different velocity profiles can be seen, especially near the load chute and the kiln bottom where the solid-bed was defined.

The gas-mixing pattern can be seen in Figure 7 for the species distribution from the load chute and the solid-bed. Because of the inward gas stream from the main burner and much reduced gas volume from the load chute, the gas from the load chute was driven toward the sludge burner side, in contrast to the flame-jet model. The gas released from the solid-bed was driven towards the kiln wall of the main burner side. This causes a poor mixing of the air from the load chute with high temperature stream from the solid-bed, and less contact with the split wastes from the broken container. Although the gas stream from the solid-bed does not represent exactly the volatilised waste, it indicates the same type of mixing.

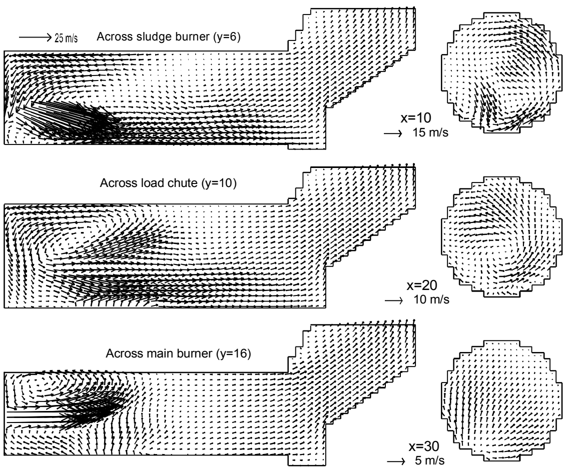

Figure 6: Velocity distribution across three inlet planes of the solid-bed model.

Turbulence model tests

In some complicated flow situations, especially for strong recirculating flows, the standard k-ε model may over-estimate the turbulence kinetic energy and viscosity in recirculations. In the absence of any flow measurement data and visualisation information, flow simulation by using a few different turbulence models may give more supports to judge the flow pattern properly. RNG and Chen-Kim k-ε models are two modified turbulence models based on the standard k-ε model, which are expected to give more accurate prediction on the recirculations and distributions of turbulence kinetic energy and viscosity.

The results from the three k-ε models indicate that the predicted maximum turbulence kinetic energy from RNG and Chen-Kim k-ε models near the incoming gas jets are lower than predicted by the standard k-ε model, as illustrated in Figure 8. However, the levels and distribution of the turbulent viscosity and the general flow patterns do not show significant differences. Table 4 lists the maximum turbulent kinetic energy and turbulent viscosity predicted with the three k-ε models. Figure 9 illustrates the velocity distribution across the kiln axis for the three turbulence models. It can be seen that the swirl above the load chute stream predicted by the RNG and Chen-Kim k-ε models is slightly larger than that from the standard k-ε model. The Chen-Kim k-ε model predicted slightly less backward flow near the outlet in the secondary combustion chamber. Similarly, a small difference is also found across the sludge and main burner planes.

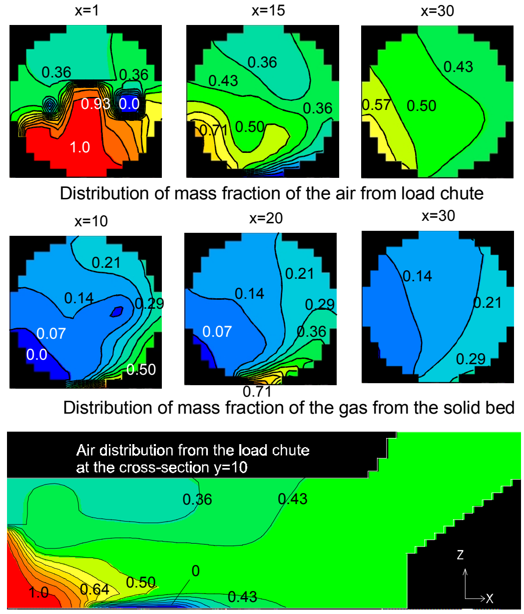

Figure 7: Species distribution of the air from the load chute, and gas from the solid-bed of the kiln.

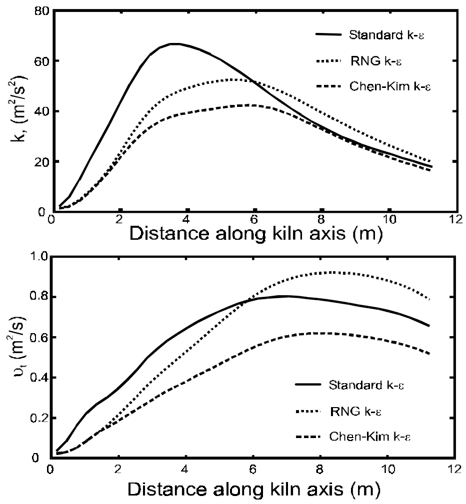

Figure 8: Distribution of turbulent kinetic energy (k) and the turbulent viscosity (ν_t) across the middle of load chute.

	Location	Standard	RNG	Chen-Kim
Max. k (m^2/s^2)	Near sludge burner	250	94	86
Max. ν_t (m^2/s)	above sludge burner jet	0.99	0.92	0.72

Table 4: Comparison of the predicted turbulent kinetic energy and turbulent viscosity.

From the turbulence model tests, it can be seen that the flow inside the kiln is highly turbulent. Due to the interaction of three flame jets, very complicated recirculating flow is formed inside the kiln. The resultant maximal turbulent viscosity is relatively high compared to the laminar viscosity (2500 to 3500 times higher).

General discussions

In the beginning of the simulation, there have been great difficulties in reaching convergence, due to the large differences of different gas streams in velocity and temperature, and a back flow from the outlet. The manipulation of the relaxation controls was not sufficient before a small wedge near the outlet was added to prevent the back flow from outside the flow domain and has improved convergence dramatically. Within 500 iterations the spot values for variables were already stable. Models were normally run for 2000 iterations and comparison with intermittent results showed very good agreement. However, model tests with including volumetric combustion heat sources were not successful due to extreme diverging problems. Definition of a smooth cylindrical kiln in the Cartesian grid system of PHOENICS is possible, but there are difficulties in defining the thermal wall boundary conditions, and therefore the traditional cell blocking technique was used. This however has shown little effect on the flow-mixing behaviour. The required computing time on a 266 MHz Pentium II is about 4 hours hour on average for 2000 iterations.

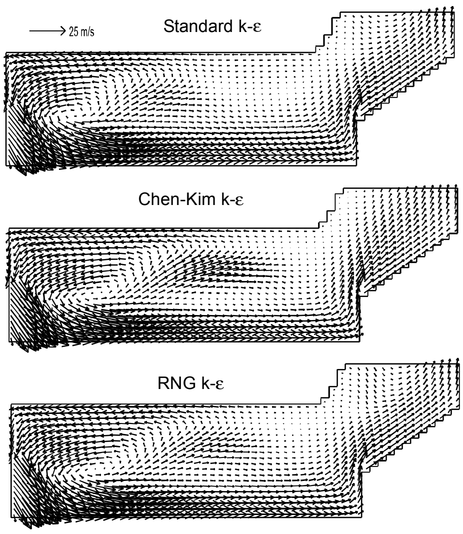

Across load chute (y=10)

Figure 9: Velocity distribution across the load chute, predicted with three k-ε models.

Field measurements of temperature and velocity are required for further development and validation of the model. The results of flow pattern and preliminary temperature distribution (adiabatic or non-adiabatic models) will be used for the field-scale temperature measurement program that is underway. The models show that the exit region of the rotary kiln is thermally non-uniform, and the temperature difference may be as high as 700°C in the solid-bed models, which is due largely to the poor mixing of different gas streams supported by the analysis of the species distribution. The flame-jet models could not give reasonable temperature distributions, because of the non-realistic inlet conditions from the load chute.

CONCLUSIONS

Based on the current studies the following conclusions can be drawn, concerning gas flow and mixing behaviour within the rotary kiln waste-incinerator at AVR Chemie:

(1) The gas flow is highly asymmetrical, three-dimensional and turbulent. The gas jet from the main burner, especially from the sludge burner, has a great effect on the air flow from the load chute, and its contact with the solid bed.

(2) Horizontal stratification of species from load chute and solid bed was predicted at the kiln exit plane, which is mainly responsible for temperature stratification.

(3) Better mixing can be expected if a more symmetric flow pattern can be arranged, and more studies are needed to test different arrangements of the burner locations and air inlets.

(4) Models of solid-bed and cold air from load chute bring more realistic representation and more accurate results than models of simple premixed and burned flame-jets.

(5) In order to predict more accurately the gas flow and mixing behaviour, radiative heat transfer and combustion modelling should be included, and this has already started.

ACKNOWLEDGEMENTS

Financial support, supply of process data, and permission to publish the data of the kiln operation from AVR Chemie are greatly acknowledged.

REFERENCES

CHAM Ltd., (1999), *PHOENICS On-Line Information System (POLIS): Lectures in PHOENICS.*

CHEN Y.S. and KIM S.W. (1987), *Computation of turbulent flows using an extended k-ε turbulence closure model*, NASA CR-179204 (from PHOENICS Encyclopedia).

JAKWAY, A. L. et al. (1996) “3-D numerical modeling of a field-scale rotary kiln incinerator”, *Environmental Science and Technology*, 30, 1699-1712.

KHAN J. A. et al. (1993), “Numerical modeling of a rotary kiln incinerator”, *Hazardous Waste and Hazardous Materials*, 10, 81-95.

LEGER, C. B. et al. (1993), “A three dimensional detailed numerical model of a field-scale rotary kiln incinerator”, *Environmental Science and Technology*, 27, 677-690.

SIGG A. (1991), “Improve combustion control in rotary kiln incinerators”, *Chemical Engineering Progress,* 87, 44-48.

SPALDING D.B. (1980), *Mathematical Modelling of Fluid Mechanics, Heat Transfer and Chemical-Reaction Processes: A Lecture Course*, Imperial College CFDU Report HTS/80/1.

VERANTH, J. M. et al. (1996), “Field investigation of the temperature distribution in a commercial hazardous waste slagging rotary kiln”, *Environmental Science and Technology*, 30, 3053-3060.

VERANTH J. M. et al. (1997), “Numerical modeling of the temperature distribution in a commercial hazardous waste slagging rotary kiln”, *Environmental Science and Technology* 31, 2534-2539.

WARDENIER, K. and VAN DEN BULCK, E. (1997) “Steady-state waste combustion and air flow optimisation in a field-scale rotary kiln”, *Environmental Engineering Science*, 14, 43-54.

YAKHOT V. et al. (1992), “Development of turbulence models for shear flows by a double expansion technique”, *Phys.Fluids A*, 4, 1510-1520.